

# Production of vector mesons by real and virtual photons at high energies

L.P.A. Haakman <sup>a</sup>, A. Kaidalov <sup>b</sup>, J.H. Koch <sup>a</sup>

<sup>a</sup> *National Institute for Nuclear Physics and High Energy Physics (NIKHEF-K),  
P.O. Box 41882, NL-1009 DB Amsterdam, The Netherlands*

<sup>b</sup> *Institute of Theoretical and Experimental Physics,  
B. Cheremushinskaya 25, 117 259 Moscow, Russia*

(24 July 1995)

A model based on Reggeon field theory is used for the description of the photo- and electroproduction of vector mesons ( $\rho^0, \omega, \phi, J/\psi$ ) on the proton. Its main feature is the dependence of the Pomeron intercept on the virtuality of the photon. The few parameters of the model were determined by fitting the total cross sections for real and virtual photons on the proton. This allows a parameter-free description of the energy dependence of vector meson production. Very good agreement with the existing high energy data is obtained.

The study of the production of vector mesons ( $\rho^0, \omega, \phi, J/\psi$ ) by real and virtual photons at high energies provides important information on the diffractive mechanism at very high energies. In particular, it allows to study the transition from the nonperturbative regime at low values of  $Q^2$ , the negative of the four momentum of the photon squared, to the perturbative regime at large  $Q^2$ . Many recent papers [1–6] have addressed the problem of the production of vector mesons. It was mainly described by the exchange of a ‘soft’ Pomeron [1,2]. At large  $Q^2$  this reaction was seen as a test of perturbative QCD and of the exchange of the so-called ‘BFKL Pomeron’ [3–6]. The new HERA data [7,8] showed a non-trivial energy dependence of the production of  $\rho^0$  and  $\psi$  mesons. The photoproduction cross section for  $\rho^0$  mesons increases slowly with energy, consistent with the soft Pomeron model of Ref. [1]. However, at high  $Q^2$  the increase is much faster than predicted by this model. This faster increase with energy is also seen for the production of  $J/\psi$ -mesons. How these high  $Q^2$  data agree with the perturbative approach or the BFKL model is not certain yet.

In this note we extend the approach in Ref. [9] to the production of vector mesons. This model was proposed for the description of the total cross section for the absorption of real and virtual photons at high energies. The central idea is that the Pomeron singularity, which governs the high energy behavior of the diffractive process, is not a simple pole characterized by a fixed intercept at  $t = 0$ ,  $\alpha_P(0)$ . Instead, multiple Pomeron exchanges must also be considered, leading to modifications of the simple pole picture. These multiple exchanges are especially important for the ‘supercritical’ Pomeron, *i.e.* when  $\Delta = \alpha_P(0) - 1 > 0$ . Single as well as multiple Pomeron exchange are actually needed to obtain an amplitude satisfying the requirements of unitarity. Diagrammatic techniques for Reggeon exchanges [10] and the AGK cutting rules [11] allow one to calculate the contributions of many such Pomeron exchanges to the scattering amplitudes and relate them to the properties of multiparticle production. Extensive phenomenological studies based on this principle (see *e.g.* Refs.[12] and [13]) have shown that all data on soft hadronic interactions can successfully be described. It follows from these analyses that the observed intercept,  $\alpha_P^{eff}(0) = 1.08$ , which characterizes the energy dependence of hadronic cross sections in the currently available range of energies,  $\sigma_{hp}^{tot} \sim s^{\alpha_P^{eff}(0)-1}$ , is substantially smaller than the intercept,  $\alpha_P(0)$ , of the single Pomeron pole itself. In the studies [12,13] which take into account sequential (‘eikonal’) many Pomeron exchanges, one finds  $\alpha_P(0) = 1.12 - 1.15$ . Taking into account a more complete set of diagrams, which also include interactions among the exchanged Pomerons, an even larger intercept of  $\alpha_P(0) \approx 1.2$  for the single pole is obtained [14].

So the *effective* intercept, which determines the overall energy dependence of the scattering amplitude, is due to the contribution from the single Pomeron exchange as well as of the Pomeron cuts, the exchanges of many Pomerons. It was argued in Ref. [9] that the relative importance of these cuts strongly decreases with the virtuality. In an electromagnetic reaction, real photons probe the entire complex of single and multiple Pomeron exchanges. However, with higher virtuality the space-time resolution increases and one ‘sees’ the single Pomeron exchange. This means that the intercept depends on  $Q^2$ , *i.e.*  $\alpha_P^{eff}(0, Q^2)$ . The exponent that governs the energy dependence of the total photon cross section thus also changes with  $Q^2$ ,  $\alpha_P^{eff}(0, Q^2) - 1 \equiv \Delta^{eff}(Q^2)$ . For real photons, at  $Q^2 = 0$ , it has the value  $\Delta^{eff}(0) \approx 0.08$  which also governs the soft hadronic interactions. At high  $Q^2$ ,  $Q^2 \gg 1 \text{ GeV}^2$ , we expect  $\Delta^{eff} \approx 0.24$  due to the Pomeron pole. The parametrization chosen in Ref. [9] was therefore

$$\Delta^{eff}(Q^2) = \Delta(0) \left( 1 + \frac{2 Q^2}{d + Q^2} \right) \quad (1)$$

with  $\Delta(0) = 0.077$  and  $d = 1.117 \text{ GeV}^2$ . At larger values of  $Q^2$  it is necessary to take into account effects due to QCD evolution, which lead to an additional increase of the energy dependence with  $Q^2$ .

The approach sketched above was applied to the electromagnetic structure function of the nucleon [9] and we compare it here to the new H1 data [18]. For values of  $Q^2$  above  $2 \text{ GeV}^2$  perturbative QCD evolution was applied on the two loop level. For the virtual photon-proton total cross section the convention is adopted that

$$\sigma_{\gamma^* p} = \frac{4\pi^2 \alpha_{EM}}{Q^2(1-x)} F_2(x, Q^2) \quad (2)$$

where  $x$  is related to the total centre-of-mass (CM) energy  $W$  by

$$W^2 \equiv s = \frac{Q^2}{x}(1-x) + m_p^2 \quad (3)$$

with  $m_p$  the mass of the proton. The results of the model from Ref. [9] are shown in Fig.1, together with the predictions for the new H1 data. The agreement with the combined experimental data is excellent. The steady increase of  $\Delta^{eff}$  with  $Q^2$  is clearly seen. As the  $Q^2$  dependence of  $\Delta^{eff}$  dies off with increasing virtuality in this model, the change in slope for values of  $Q^2 \gg d$  is due to the QCD evolution. We also show a cross section for a low virtuality,  $Q^2 = 0.35 \text{ GeV}^2$ , which can be compared with the forthcoming data from E665. The preliminary data [19] indicate that our model also works very well in the kinematical range covered by E665.

The same approach can be used for other diffractive processes, such as the production of vector mesons by real as well as virtual photons,  $\gamma^{(*)} p \rightarrow V p$ . The combined contribution of the Pomeron pole and the cuts to the amplitude for this process can be written in the following form

$$T(s, t, Q^2, m_V^2) = f(Q^2, m_V^2, t) \left( \frac{s}{s_0} \right)^{\alpha_P^{eff}(t, \bar{Q}^2)} \eta(\alpha_P^{eff}) \quad (4)$$

where  $\eta(\alpha)$  is the signature factor and the dependence on the total CM-energy is determined by the effective Pomeron trajectory with  $\alpha_P^{eff}(t, \bar{Q}^2)$ . We have indicated through the argument  $\bar{Q}^2$  that this effective parameter depends on the characteristic virtuality of the process. For the production of states made up of light quarks ( $u, d, s$ ) we have  $\bar{Q}^2 = Q^2$ , while for vector mesons made up of heavy quarks we choose

$$\bar{Q}^2 = c m_q^2 + Q^2 \quad (5)$$

where  $m_q$  is the mass of the heavy quark and  $c \sim 1$ . In this way we take into account that for production of states made up of heavy quarks the contribution of cuts is small already at low  $Q^2$ . The effective pomeron trajectory  $\alpha_P^{eff}(t, \bar{Q}^2)$  is assumed to be linear in  $t$ , *i.e.*

$$\alpha_P^{eff}(t, \bar{Q}^2) = 1 + \Delta^{eff}(\bar{Q}^2) + \alpha'_P t \quad (6)$$

with the same parametrization for  $\Delta^{eff}(\bar{Q}^2)$ , Eq.(1), as in the structure function of the proton in Ref. [9]. We take  $\alpha'_P = 0.25 \text{ GeV}^{-2}$ , which was obtained from the analysis of hadronic interactions. In principle  $\alpha'_P$  also depends on  $\bar{Q}^2$ , but from analysis of elastic hadronic reactions it follows that this dependence is rather weak and can be neglected when discussing the energy dependence of the cross section. The  $t$ -dependence of the function  $f(Q^2, m_V^2, t)$  is well known from *e.g.* proton scattering,  $\pi N$  scattering and the production of  $\rho^0$  mesons on the proton at low energies. It is taken to be exponential [1],

$$f(Q^2, m_V^2, t) = \tilde{f}(Q^2, m_V^2) \exp(R^2 t) \quad (7)$$

with  $R^2 = R_p^2 + R_V^2(Q^2)$  where

$$\begin{aligned} R_V^2 &= \frac{R_{0V}^2 m_\rho^2}{m_V^2 + Q^2} \\ R_p^2 &= 2 \text{ GeV}^{-2} \\ R_{0V}^2 &= R_\rho^2 = 1 \text{ GeV}^{-2} \quad . \end{aligned} \quad (8)$$

It has a factorizable form and takes into account the change with  $Q^2$  and  $m_V^2$  of the radius of the  $\gamma VP$  vertex.

The contribution of the Pomeron to the differential cross section for the  $\gamma^{(*)}p \rightarrow Vp$  reaction then becomes

$$\frac{d\sigma}{dt} = \frac{1}{16\pi s^2} |T(s, t, Q^2, m_V^2)|^2 = \mathcal{F}(Q^2, m_V^2) \left( \frac{s}{s_0} \right)^{2\Delta^{eff}(Q^2)} \exp(\Lambda(s)t) \quad (9)$$

where

$$\mathcal{F}(Q^2, m_V^2) = \frac{|\tilde{f}(q^2, m_V^2) \eta(\alpha_P)|^2}{16\pi} \quad (10)$$

and

$$\Lambda(s) = 2 \left( R^2 + \alpha'_P \ln\left(\frac{s}{s_0}\right) \right) \quad (11)$$

is the slope of the diffraction cone. For the scale factor,  $s_0$ , we choose  $s_0 = m_V^2 + Q^2$ . This can be done, since the function  $\mathcal{F}(Q^2, m_V^2)$  is unknown and will be fitted to the data. The dependence on the energy  $s$  is however entirely determined from Eqs.(1) and (9). The cross section due to Pomeron exchange, Eq. (9), can then be written as

$$\frac{d\sigma}{dt} = \Phi(Q^2, m_V^2) (F_{2,p}^{sea}(x, \bar{Q}^2)^2 \exp(\Lambda(s)t) \quad (12)$$

where  $F_{2,p}^{sea}(x, \bar{Q}^2)$  is the sea quark contribution to the structure function of the proton [9] with  $x = \bar{Q}^2/(\bar{Q}^2 + s)$ . Eq.(12) allows us to include perturbative QCD corrections, which are important at large values of  $Q^2$ , by applying the QCD evolution equations to the structure function. For the production of vector mesons made up of  $u$  and  $d$  quarks ( $\rho^0, \omega$ ), at not too large energies also secondary exchanges — the  $f$  and  $A_2$  Regge poles — contribute in addition to the Pomeron exchange. In the parametrization of the structure function  $F_2^p(x, Q^2)$  in Ref. [9] they correspond to the valence quark contribution. In the following we shall assume that for ( $\rho^0, \omega$ )–production the ratio of the Pomeron to secondary exchanges is the same as for the structure function. This means that the entire structure function  $F_2^p$  as parametrized in Ref. [9] enters into Eq.(12) for vector meson production.

Results for the total cross section for the reaction  $\gamma^* p \rightarrow \rho^0 p$ , obtained by integrating Eq.(12) over  $t$ , are shown in Fig.2. At each value of  $Q^2$ , the curves are normalized to obtain a good fit to the data. For energies where we expect our Reggeon-based model to apply,  $s > 10 \text{ GeV}^2$ , the data are described well. Especially the strong increase of the cross section with energy that was observed by the ZEUS Collaboration [7] at  $Q^2 \sim 10 \text{ GeV}^2$  is well reproduced by the model. It will be interesting to test the model predictions for high energies, in particular at lower values of  $Q^2$ .

The data for  $\omega$ –meson photoproduction are shown in Fig.3 . Only relatively low energy data are available and their  $W$  dependence is well described. For the photoproduction of  $\phi$  and  $J/\psi$  mesons there is no valence quark contribution and only Pomeron exchange contributes to the amplitude. Using for the charmed quark mass  $m_c^2 = 2.6 \text{ GeV}^2$ , we obtain good agreement with recent HERA results [8] as shown in Fig.3 . The energy dependence of the  $\phi$  meson is weaker and is also well reproduced by the model.

In conclusion, the data on photo- and electroproduction of vector mesons yield additional support for the idea of a steady change of the effective intercept of the Pomeron singularity. The simple model based on this idea can be used to predict the energy dependence for other diffractive processes in photo- and electroproduction at high energies.

## ACKNOWLEDGEMENT

The work of L.H. and J.K. is part of the research program of the Foundation for Fundamental Research of Matter (FOM) and the National Organization for Scientific Research (NWO). The collaboration with ITEP is supported in part by a grant from NWO and by grant 93-79 of INTAS. A.K. also acknowledges support from grant J74100 of the International Science Foundation and the Russian Government.

- 
- [1] A. Donnachie, P.V. Landshoff, Phys. Lett. **B185** (1987) 403; A. Donnachie, P.V. Landshoff, Phys. Lett. **B348** (1995) 213
  - [2] J. R. Cudell, Nucl. Phys. **B336** (1990) 1
  - [3] M.G. Ryskin, Z. Phys. **C57** (1993) 89
  - [4] J.R. Forshaw and M.G. Ryskin, DESY 94-162
  - [5] J. Nemchik, N.N. Nikolaev and B. Zakharov, Phys. Lett. **B341** (1994) 228
  - [6] S.J. Brodsky, L. Frankfurt, A.H. Mueller, M. Strikman, Phys. Rev. **D50** (1994) 3134
  - [7] ZEUS Collaboration, DESY Report 95-133 (1995)
  - [8] M. Derrick *et al.* (ZEUS Collaboration), Phys. Lett. **B350** (1995) 120
  - [9] A. Capella, A. Kaidalov, C. Merino and J. Tran Thanh Van, Phys. Lett. **B337** (1994) 358
  - [10] V.N. Gribov, ZhETF **57** (1967) 654
  - [11] V.A. Abramovski, V.N. Gribov and O. Kancheli, Sov. J. Nucl. Phys. **18** (1974) 308
  - [12] A. Kaidalov in “QCD at 200 TeV”, edited by L. Cifarelli and Yu. Dokshitzer, Plenum Press (1992) 1
  - [13] A. Capella, U. Sukhatme, C.-I. Tan and J. Tran Thanh Van, Phys. Rep. **236** (1994) 225
  - [14] A. Kaidalov, L. Ponomarev and K.A. Ter-Martirosyan, Sov. J. Nucl. Phys. **44** (1986) 468

- [15] A compilation of  $F_2$  data from BCDMS, NMC, SLAC and ZEUS can be found *e.g.* in Refs. [9] and [18]
- [16] S.I. Alekhin *et al.*, CERN-HERA Report 87-01
- [17] T. Ahmed *et al.* (H1 Collaboration), Phys. Lett. **B299** (1992) 374; M. Derrick *et al.* (ZEUS Collaboration), Phys. Lett **B293** (1992) 465
- [18] T. Ahmed *et al.* (H1 Collaboration), Nucl. Phys. **B439** (1995) 471
- [19] A. Kotwal (E665 Collaboration), Talk at the Workshop “The Heart of Matter”, Blois, France, June 1994

## FIGURE CAPTIONS

**Fig.1** The total cross sections for real and virtual photons for the proton obtained from the model of Ref. [9]. Reading from top to bottom the curves belong to :  $Q^2 = 0, 0.35, 1.4, 3, 8.5, 15, 35, 65, 125 \text{ GeV}^2$ . The H1 data [18] are denoted by the black squares , the ZEUS data [15] by the open circles and the low energy data from BCDMS, SLAC and NMC [15] by the open triangles. The real photon data [16–17] are indicated by the open squares.

**Fig.2** The  $\gamma^* p \rightarrow \rho^0 p$  cross sections for several values of  $Q^2$  obtained from our model. The data for  $W > 50 \text{ GeV}$  at high  $Q^2$  are the recent ZEUS-data. All data are from [7] and references therein.

**Fig.3** A compilation of total photoproduction and vector meson production cross sections resulting from the model. The high energy data are from Refs. [7], [8] and [17]. The low energy data are from [16] and references in [8].

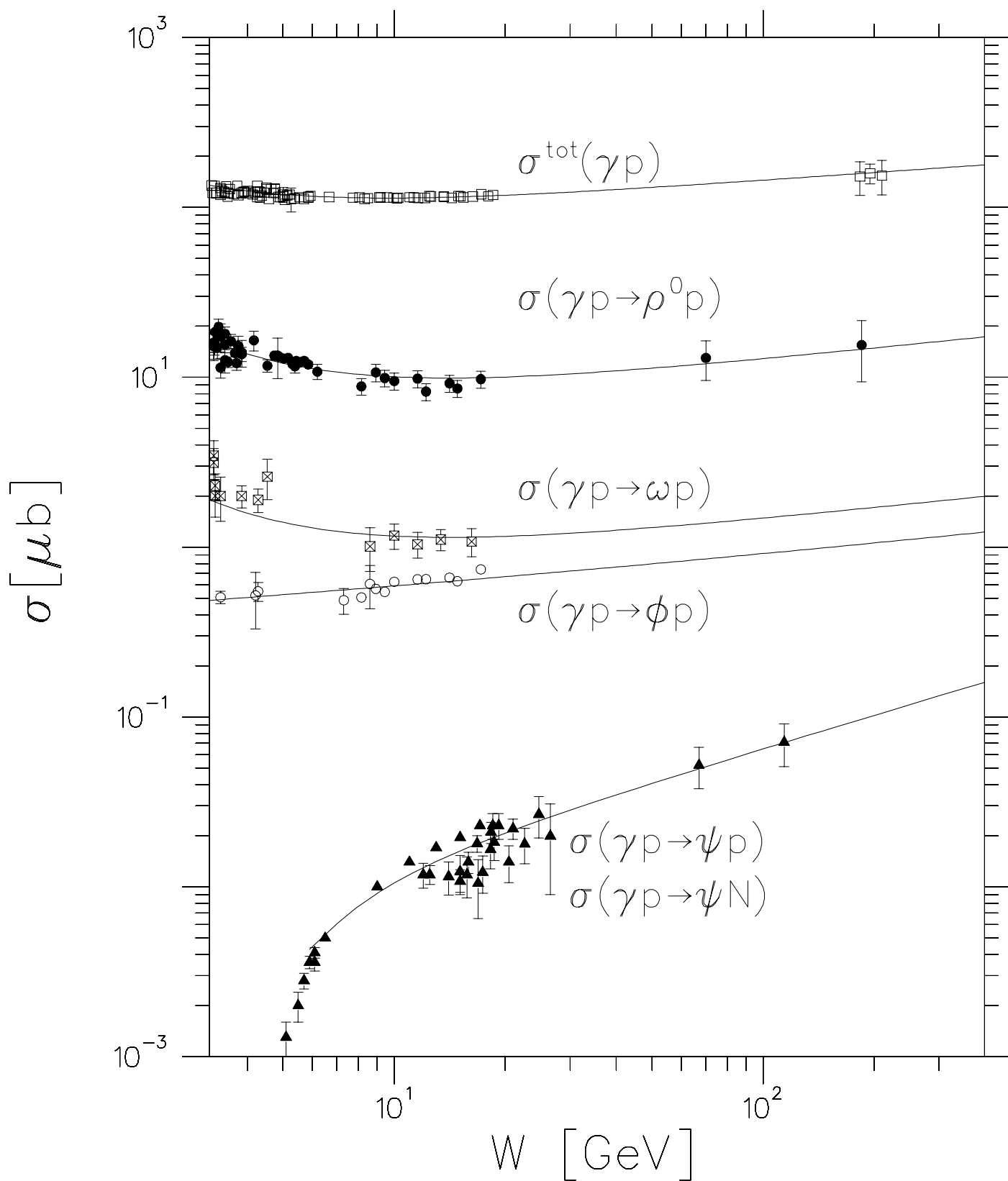


Fig.3

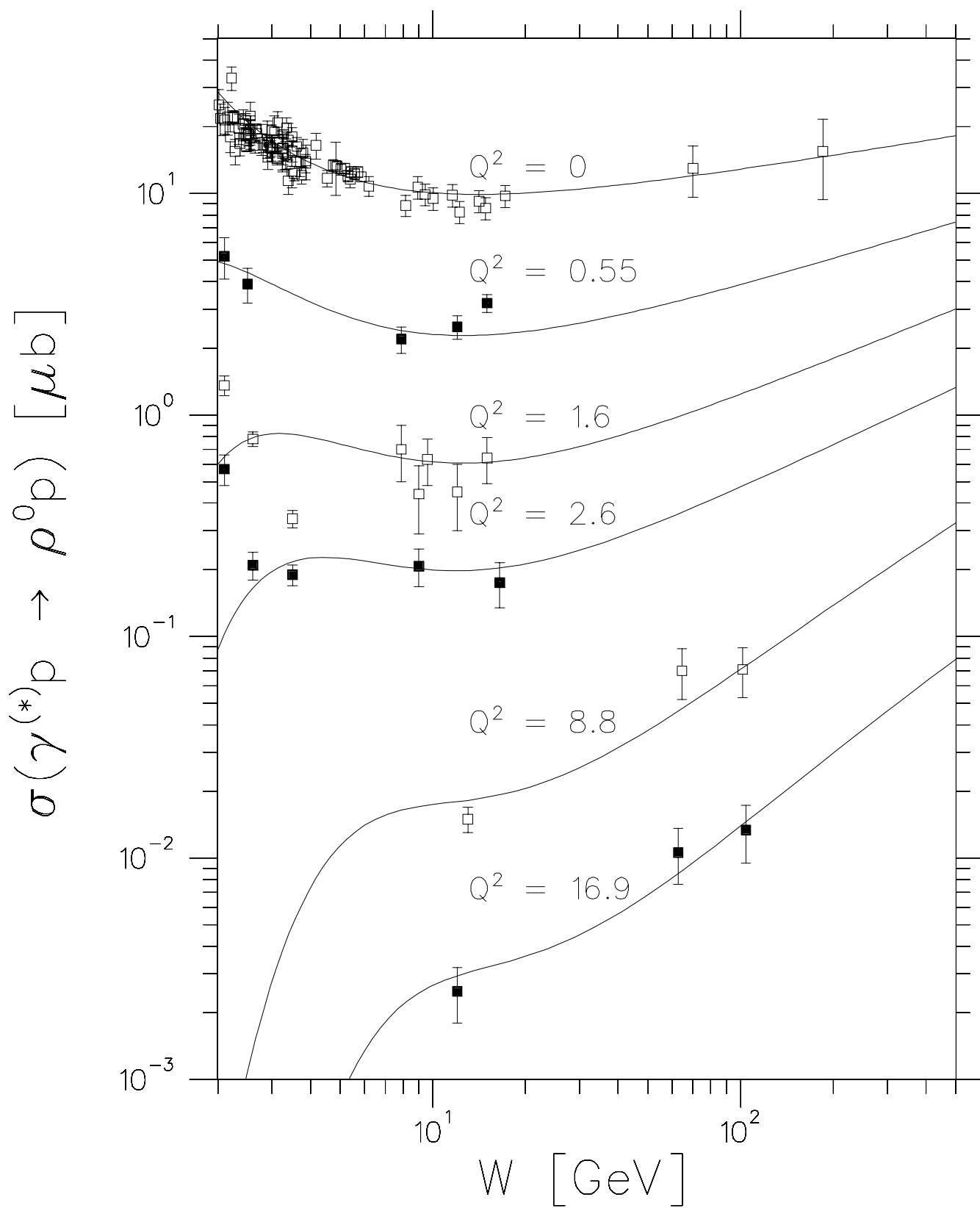


Fig.2

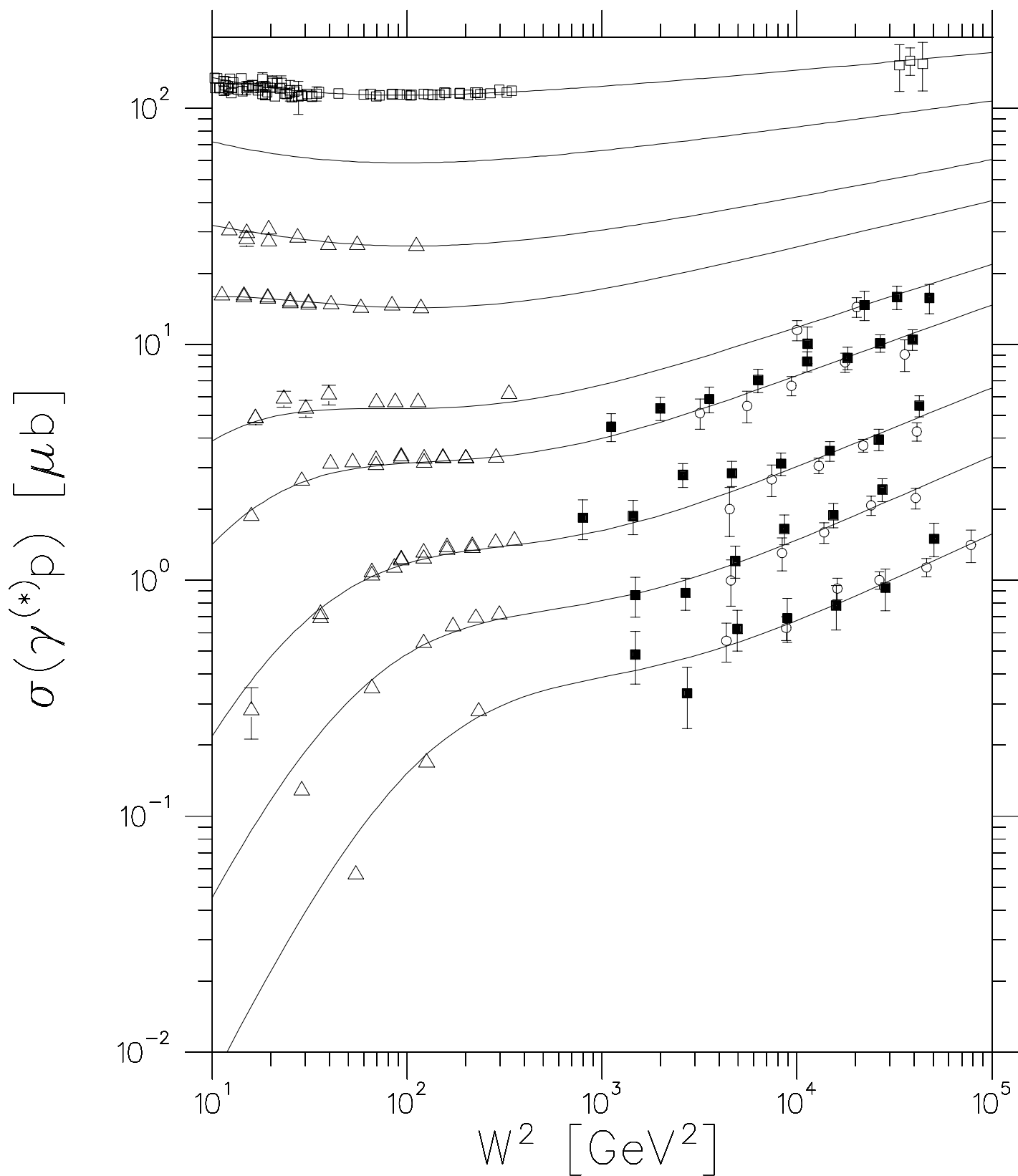


Fig.1